JPET Fast Forward. Published on August 6, 2013 as DOI: 10.1124/jpet.113.205138
This article has not been copyedited and formatted. The final version may differ from this version.

JPET #205138

Enhancement of Ca^{2+} influx and ciliary beating by membrane hyperpolarization due to ATP-sensitive K^+ channel opening in mouse airway epithelial cells

Teruya Ohba, Eiji Sawada, Yoshiaki Suzuki, Hisao Yamamura,

Susumu Ohya, Hiroyuki Tsuda and Yuji Imaizumi

Department of Molecular and Cellular Pharmacology, Graduate School of Pharmaceutical Sciences, Nagoya City University, Nagoya, Japan (TO, ES, YS, HY, YI)

Department of Pharmacology, Division of Pathological Sciences, Kyoto Pharmaceutical University, Kyoto, Japan (SO)

Nanomaterial Toxicology Project, Nagoya City University, Nagoya, Japan (HT)

a) Running title: K^+ channel opening facilitates ciliary movement

b) Correspondence author: Yuji Imaizumi, Ph.D.

Department of Molecular and Cellular Pharmacology

Graduate School of Pharmaceutical Sciences

Nagoya City University

3-1 Tanabedori, Mizuhoku, Nagoya 467-8603, Japan

TEL & FAX: +81-52-836-3431

E-mail: yimaizum@phar.nagoya-cu.ac.jp

c) Manuscript: 24 pages, 0 tables, 6 figures, and 34 references. Abstract (243 words), Introduction (473 words), and Discussion (1481 words).

d) Abbreviations: $[Ca^{2+}]_i$, intracellular Ca^{2+} concentration; CBF, ciliary beating frequency; DPBS, Dulbecco's phosphate-buffered saline; fluo-4/AM, fluo-4 acetoxymethyl ester; fura-2/AM, fura-2 acetoxymethyl ester; K_{ATP} channel, ATP-sensitive K^+ channel; VDCC, voltage-dependent Ca^{2+} channel.

e) Section: Respiratory

JPET Fast Forward. Published on August 6, 2013 as DOI: 10.1124/jpet.113.205138
This article has not been copyedited and formatted. The final version may differ from this version.

Abstract

Among the several types of cells composing the airway epithelium, the ciliary cells are responsible for one of the most important defense mechanisms of the airway epithelium: the transport of inhaled particles back up into the throat by coordinated ciliary movement. Changes in the cytoplasmic Ca^{2+} concentration ($[Ca^{2+}]_i$) are the main driving force controlling the ciliary activity. In mouse ciliary cells, membrane hyperpolarization from -20 to -60 mV under whole cell voltage-clamp induced a slow but significant $[Ca^{2+}]_i$ rise in a reversible manner. This rise was completely inhibited by the removal of Ca^{2+} from the extracellular solution. Application of diazoxide, an ATP-dependent K^+ channel opener, dose-dependently induced a membrane hyperpolarization (EC_{50} = 2.3 μM), which was prevented by the addition of 5 μM glibenclamide. An inwardly rectifying current was elicited by the application of 10 μM diazoxide and suppressed by subsequent addition of 5 μM glibenclamide. Moreover, the application of 10 μM diazoxide induced a significant $[Ca^{2+}]_i$ rise and facilitated ciliary movement. Multi-cell RT-PCR analyses and immunocytochemical staining suggested that the subunit combination of Kir6.2/SUR2B and possibly also Kir6.1/SUR2B is expressed in ciliary cells. The confocal Ca^{2+} imaging analyses suggested that the $[Ca^{2+}]_i$ rise induced by diazoxide occurred preferentially in the apical submembrane region. In conclusion, the application of a K_{ATP} channel opener to airway ciliary cells induces membrane hyperpolarization and thereby induces a $[Ca^{2+}]_i$ rise via the facilitation of Ca^{2+} influx through the non-voltage dependent Ca^{2+} permeable channels. Therefore, a K_{ATP} opener may be beneficial in facilitating ciliary movement.

JPET Fast Forward. Published on August 6, 2013 as DOI: 10.1124/jpet.113.205138
This article has not been copyedited and formatted. The final version may differ from this version.

Introduction

The regulation of K^+ channel conductance is suggested to be a critical issue in the therapy of asthma and/or chronic obstructive pulmonary disease (Pelaia et al., 2002; Malerba et al., 2010). The activation of the ATP-sensitive K^+ (K_{ATP}) channel, the large conductance Ca^{2+} activated K^+ (BK) channel, or the intermediate conductance Ca^{2+} activated K^+ (IK) channel by specific modulators induces the following: bronchodilation, a reduction in the hyper-responsiveness of the airways, a reduction in mucus production, a reduction in cough, the suppression of airway inflammation, and the remodeling of the preclinical models of asthma and chronic obstructive pulmonary disease (Malerba et al., 2010).

Ciliary cells play a fundamental role in the airway self-defense system by removing foreign materials from the airways in functional combinations with the other types of epithelial cells. The motile cilia in the airway epithelium are the engines for mucociliary clearance, which is a mechanism responsible for cleaning the airways of inhaled particles. The ciliary beating observed in the human airway epithelium is principally due to a slow constitutive rate of beating caused by inherent and spontaneous dynein ATPase activity. The cilia can increase their beating frequency by the activation of several different control mechanisms, one of these being changes in the intracellular Ca^{2+} concentration ($[Ca^{2+}]_i$) (Evans and Sanderson, 1999; Schmid and Salathe, 2011). Aside from the regulatory effects of calcium on the ciliary beating rate, calcium is also involved in the complex task of synchronizing the beat among the cilia of one single cell as well as between the cilia on multiple cells (Schmid and Salathe, 2011).

Initially, K_{ATP} channels were identified as the key molecules for insulin secretion in pancreatic β-cells and are now well known to be ubiquitously expressed in a variety of tissues as the molecular combination of channel-forming Kir6.x subunits and sulfonylurea receptors (SURs) (Clark and Proks, 2010; Flagg et al., 2010; Hibino et al., 2010). While the expression of K_{ATP} channels has been reported in alveolar cells (Trinh et al., 2007) and cell lines derived from human

airway epithelial tissues (Trinh et al., 2008), their functional expression in ciliary cells has not yet been documented. Previous studies have revealed that ATP and acetylcholine are major endogenous stimulants that facilitate ciliary beating by activating the purinoceptors and by increasing $[Ca^{2+}]_I$, which, in turn, may induce membrane hyperpolarization via the activation of Ca^{2+}-dependent K^+ channels (Weiss et al., 1992; Tarasiuk et al., 1995). However, conflicting reports have been published as to whether changes in the membrane potential can significantly impact the ciliary beat frequency (Ma et al., 2002). Therefore, the present study was undertaken to elucidate the effects of K_{ATP} openers on ciliary beating rates and to determine the underlying mechanisms of the changes. The effects of K_{ATP} openers on ciliary beating may be a key issue in evaluating their therapeutic potentials for respiratory diseases.

Materials and Methods

Animals

C57BL/6N male mice (Japan SLC, Hamamatsu, Japan), 8-12 weeks old, were used. All experiments were carried out in accordance with the Guiding Principles for the Care and Use of Laboratory Animals of the Japanese Pharmacological Society and also with the approval of the Ethics Committee of Nagoya City University.

Isolation of single ciliary cells

The tracheas were removed from the mice. The epithelium was separated from the cartilage and cut into squares of approximately 1 x 1 mm. The tissue was maintained in Dulbecco's phosphate-buffered saline (DPBS) containing (in mM): 137 NaCl, 2.7 KCl, 0.9 $CaCl_2$, 0.5 $MgCl_2$, 8 Na_2HPO_4, 1.47 KH_2PO_4, and 5 glucose (pH 7.4). The epithelium was incubated for 25 min at 37°C in DPBS supplemented with 13 U/ml papain (Sigma-Aldrich, St. Louis, MO), 1 mg/ml bovine serum albumin (BSA) (Sigma-Aldrich), and 1 mg/ml 1,4-dithiothreitol (Wako Pure Chemicals,

Osaka, Japan). Following incubation, the solution was replaced with DPBS. The cells were then dispersed several times with a fire-polished Pasteur pipette. The isolated cells were immediately used following the cell dispersion. All of the experiments were carried out at room temperature (25°C).

Multi-cell RT-PCR

About 40 ciliary cells were collected by the glass electrode of 20~30 μm in diameter. Total RNA was extracted from them using NucleoSpin RNA XS (MACHEREY NAGEL, Düren, Germany) and reverse transcribed using oligo$(dT)_{12-18}$ primer and SuperScript II reverse transcriptase (Invitrogen, Carlsbad, CA). The solution without RNase was used as a negative control. The PCR amplification profile using KOD-Plus-Neo (TOYOBO, Tokyo, Japan) and GeneAmp PCR System 2700 (Applied Biosystems) was as follows: a 10-s denaturation step at 98°C, a 30-s annealing step at 55°C and, a 60-s primer extension step at 72°C for 35 cycles. Gene products were analyzed by 2.0% agarose gel electrophoresis.

PCR primers

The following PCR primers were used: for mouse Kir6.1/Kcnj8 (GenBank Accession No. NM_008428), (+) 5'-CAA GTG ACC ATT GGG TTT GGA-3' and (-) 5'-CGT TGA TGA TCA GAC CCA CGA-3' (100 bp); Kir6.2/Kcnj11 (NM_010602), (+) 5'-CAA GAA AGG CAA CTG CAA CGT-3' and (-) 5'-TGT GTG GCC ATT TGA GGT CCA-3' (101 bp); SUR1/Abcc8 (NM_011510), (+) 5'-AGT GAA GCC CCC TGA GGA CCT-3' and (-) 5'-GAT GAA GGC ATT CAT CCA CCA-3' (103 bp); SUR2/Abcc9 (NM_021041 and NM_011511), (+) 5'-TAC GAA CAT CAT CGA CCA GCA-3' and (-) 5'-AAA CAC GGG TGT AGC ATA GGA-3' (109 bp); β-actin/Actb (NM_007393), 5'-AGG CCA ACC GTG AAA AGA TG-3' and (-) 5'-ACC AGA GGC ATA CAG GGA CA-3' (101 bp). The specific primers for the spliced variant analysis of

SUR2 were designed as follows: for mouse SUR2A/Abcc9A (NM_021041), (+) 5'-TCT TCT ATT GTG GAT GCA GGC CT-3' and (-) 5'-CTA CTT GTT GGT CAT CAC CAA AGT-3' (129 bp); SUR2B/Abcc9B (NM_011511), (+) 5'-CAC ACC ATT CTG ACT GCA GAC CT-3' and (-) 5'-TCA CAT GTC TGC ACG GAC AAA CGA-3' (129 bp).

Immunocytochemistry

Polyclonal anti-mouse Kir6.2 (APC-020) and control antigen were purchased from Alomone Labs (Jerusalem, Israel). Polyclonal antibodies to Kir6.1 (R-14), SUR1 (H-80), SUR2A (M-19), SUR2B (C-15) and each blocking peptide were purchased from Santa Cruz Biotechnology, inc. (Dallas, TX). Dissociated ciliary cells were settled down on coverslipes precoated with poly-L-lysin (Matsunami). These cells were fixed with 4% paraformaldehyde for 20 min and permeabilized with 0.2% Triton/PBS for 15 min at room temperature. After rinsing in PBS containing 1% normal goat serum (NGS), the cells were pre-incubated for 1 hr with 10% NGS/PBS to minimize non-specific binding of antibodies, and incubated successively with 1:100 diluted antibodes for 12 hr. Primary antibodes were extensively washed with 1% NGS/PBS, and incubated with Alexa 488-conjugated anti-rabbit IgG goat or Alexa 488-conjugated anti-goat IgG rabbit antiserum (Molecular Probe, Eugene, OR) for 1 hr. Immunostained cells were observed using a laser scanning confocal fluorescent microscope (A1R, Nikon, Tokyo, Japan) equipped with a fluorescent microscope (ECLIPSE Ti, Nikon), an objective lens (Plan Apo 60× 1.40 NA, oil immersion, Nikon), and NIS Elements software (version 3.10, Nikon). The excitation wavelength from the multi-argon laser (Melles Griot, Carlsbad, CA) for Alexa 488 was 488 nm and the emission light was collected by a band-pass filter (525/50 nm).

Electrophysiological recordings

A whole cell patch clamp was applied to a single ciliary cell with a patch pipette using a CEZ-2400 amplifier (Nihon Kohden, Tokyo, Japan) as previously described (Imaizumi et al., 1989; Yamamura

et al., 2012). The membrane currents and voltage signals were stored and analyzed using a Digidata 1440A and a pCLAMP 10.2 (Axon Instruments, Foster City, CA). The ciliary cells were clamped at a holding potential of -40 mV, and a descending ramp protocol from +40 to -120 mV for 500 ms was performed every 10 s. In some experiments, membrane potentials from single ciliary cells were measured under the current clamp mode in whole cell configuration.

Measurement of the Ca^{2+} fluorescence ratio and the Ca^{2+} images

The airway ciliary cells were loaded with 10 μM fura-2 acetoxymethyl ester (fura-2/AM, Molecular Probes) in a standard HEPES solution for 45 min at room temperature. The fura-2 fluorescent signals were measured using the Argus/HiSCA imaging system (Hamamatsu Photonics, Hamamatsu, Japan). In some experiments, in which simultaneous measurements of $[Ca^{2+}]_i$ and membrane potential were taken, ciliary cells were loaded with 100 μM fluo-4 (Molecular Probes) by diffusion from the recording pipette (Funabashi et al., 2010). The Ca^{2+} images were scanned every 2 s.

Intracellular Ca^{2+} images by use of fluo-4/AM and confocal fluorescent microscopy

The airway ciliary cells were loaded with 10 μM fluo-4 acetoxymethyl ester (fluo-4/AM, Molecular Probes) in a standard HEPES solution for 45 min at room temperature. The cytosolic Ca^{2+} images were obtained using a laser scanning confocal fluorescent microscope and NIS Elements software mentioned above. The excitation wavelength for fluo-4 was 488 nm and the emission wavelength was collected by a band-pass filter (525/50 nm). The resolution of the microscope was 0.414 μm per pixel and 2.02 μm to the Z-axis direction. The confocal images were scanned over a full frame (512×512 pixels) every 2 s.

Membrane potential measurements by voltage-sensitive fluorescent dye

The membrane potential was measured as previously reported (Yamazaki et al., 2011) using 100 nM $DiBAC_4(3)$ (Dojin, Kumamoto, Japan), a bis-barbituric acid oxonol dye with an excitation maximum at approximately 488 nm. The data were collected and analyzed using the ARGUS/HiSCA imaging system. The sampling interval of the $DiBAC_4(3)$ fluorescence measurements was every 5 s.

Measurement of CBF

The ciliary beating frequency (CBF) of the tracheal airway ciliary cell (Shiima-Kinoshita et al.2004; Kawakami et.al. 2004) was measured at 100 Hz using a high-speed resolution CCD camera (C9100-12, Hamamatsu Photonics). Prior to the experiments, the CBFs were measured every 1 minute for 2 min and the average value of these three CBFs were used as the basal CBF (CBF_0) in the HEPES-buffered solution. Any changes in the CBF were expressed as a CBF ratio.

Solutions

An extracellular solution was made using a standard HEPES-buffered solution composed of the following (in mM): 137 NaCl, 5.9 KCl, 2.2 $CaCl_2$, 1.2 $MgCl_2$, 14 glucose, and 10 HEPES. The pH of the solution was adjusted with NaOH to 7.4. The K_{ATP} current was measured in a 40 mM K^+ HEPES-buffered solution composed of the following (in mM): 99.7 NaCl, 40 KCl, 2.2 $CaCl_2$, 1.2 $MgCl_2$, 14 glucose, and 10 HEPES. The pH of the solution was adjusted with NaOH to 7.4. The pipette solution for electrical recordings contained the following (in mM): 140 KCl, 4 $MgCl_2$, 2 ATP-Na_2, 0.05 EGTA, 10 HEPES. The pH of the solution was adjusted with KOH to 7.2. All experiments were undertaken at room temperature to avoid fura-2 trapping in organelles and dye leakage at 37 ^oC.

Statistical analysis

JPET Fast Forward. Published on August 6, 2013 as DOI: 10.1124/jpet.113.205138
This article has not been copyedited and formatted. The final version may differ from this version.

The pooled data are expressed as means ± SE, and the statistical significance was examined using Student's *t*-test for two groups and Tukey's for three or more groups. P values <0.05 were considered statistically significant. The data of the relationship between diazoxide and fluorescent signal were fitted using the following equation after normalization: $F/F_0 = 1-(1-C)/\{1+(K_d/<diazoxide>)^n\}$, where C is the component resistant, K_d is the apparent dissociation constant, <diazoxide> is the concentration, and n is the Hill coefficient (Fig. 2B,b).

Drugs

The pharmacological reagents were obtained from Sigma-Aldrich. Diazoxide, glibenclamide, and pinacidil were dissolved in dimethyl sulfoxide (DMSO) at concentrations of 5 to 10 mM as a stock solution.

Results

The effects of K_{ATP} opener on ciliary beating

The ciliary movement in freshly isolated mice ciliary cells was recorded at 100 Hz using a high time-resolution video camera and analyzed using a slow image reproduction (Fig. 1A). The application of 10 μM diazoxide, a K_{ATP} channel opener, significantly increased the frequency of the ciliary movement (Fig. 1B) and the effect lasted for over 10 min (not shown). The addition of 5 μM glibenclamide, a K_{ATP} channel blocker, removed the diazoxide-induced enhancement of the frequency (Fig. 1B). The summarized data (Fig. 1C) indicate a significant enhancement of the frequency when 10 μM diazoxide was applied (n=6, $p<0.05$ vs. control) and a significant inhibition of the frequency when 5 μM glibenclamide was added (n=6, $p<0.01$ vs. diazoxide alone). Although the amplitude of the movement may also be increased by the diazoxide, those quantitative analyses could not be done during this study due to the limited time resolution of the video system.

JPET Fast Forward. Published on August 6, 2013 as DOI: 10.1124/jpet.113.205138
This article has not been copyedited and formatted. The final version may differ from this version.

The K_{ATP} opener–induced membrane hyperpolarization and the subsequent rise in $[Ca^{2+}]_i$

The membrane potential changes induced by the addition of 10 μM diazoxide in the isolated ciliary cells were measured using the voltage sensitive fluorescent dye $DiBAC_4(3)$.

The sustained decrease in the fluorescence intensity observed following the addition of 10 μM diazoxide is indicative of membrane hyperpolarization (n=5, $p<0.01$). The diazoxide-induced decrease in fluorescence intensity was completely removed by the addition of 5 μM glibenclamide (n=5, $p<0.01$; Fig. 2A). The diazoxide-induced decrease in fluorescence intensity was concentration-dependent in the range of 1 and 30 μM (Fig. 2B). The EC_{50} value for membrane potential of the cells treated with diazoxide was 2.3 μM and the Hill coefficient was 3.4 (n=11).

The membrane potential was also measured under current clamp mode in freshly isolated single ciliary cells using pipette filling solution containing 140 mM KCl (see Methods). In all four experiments, in which stable recordings for over 10 min were successfully obtained throughout the procedure to add two drugs sequentially, the addition of 10 μM diazoxide induced sustained membrane hyperpolarization of 3.6±1.4 mV from the resting membrane potential of -18.6±1.4 mV (n=4). Further addition of 5 μM glibenclamide resulted in depolarization by 2.4±0.5 mV (n=4). Taking the initial resting membrane potential in each cell as 1.0, the potentials after the addition of diazoxide and glibenclamide were 1.20±0.03 ($p<0.01$ vs. 1.0) and 1.07±0.03 ($p<0.05$ vs. glibenclamide alone).

The effects of the diazoxide on $[Ca^{2+}]_i$ were examined in isolated ciliary cells using fura-2/AM (Fig. 3A). The application of 10 μM diazoxide increased the fluorescence ratio (F340/F380), indicating the increase in $[Ca^{2+}]_i$ (n=8, $p<0.01$). This observed increase was removed by the addition of 5 μM glibenclamide (n=5, $p<0.01$). The $[Ca^{2+}]_i$ was also increased by the application of 10 μM pinacidil, another K_{ATP} channel opener (n=5, $p<0.01$) and the effect was again reversed by the addition of 5 μM glibenclamide (n=5, $p<0.01$).

The expression of ATP-sensitive K^+ channels in ciliary cells

The molecular characteristics of the K_{ATP} channels in the ciliary cells were examined by multi-cell RT-PCR analysis. These analyses reveal that the transcripts of Kir6.2 and SUR2B were predominantly expressed in the ciliary cells (n=3; Fig. 4A).

To clarify protein expression of these channels, immunocytechemical analyses were performed (n=3; Fig. 4B). Kir6.1, Kir6.2 and SUR2B proteins were detected on plasma membrane of ciliary cells. However, SUR2A did not show significant membrane surface expression. These results are consistent with those from RT-PCR analyses and strongly suggest that Kir6.2/SUR2B and possibly also Kir6.1/SUR2B are predominantly expressed in mouse ciliary cells. It was unexpected finding that SUR1 showed specific expression on cilia.

The mesurement of ATP-sensitive K^+ channel currents in ciliary cells

The K_{ATP} channel current was measured in a single ciliary cell using a whole cell patch-clamp recording. To amplify the conductance of the Kir channel, the recordings were performed in an external solution containing 40 mM K^+. The current-voltage relationship in the control showed slight inward rectification at potentials negative to -60 mV. The inwardly rectifying current was markedly enhanced by the application of 10 μM diazoxide (Fig. 5A). The enhanced current was reduced by the addition of 5 μM glibenclamide. The reversal potential of the current component reduced by glibenclamide in the presence of diazoxide was -33 mV, which is close to the equilibrium potential of K^+ under the conditions (E_K = -32 mV). The summarized data (Fig. 5B) clearly indicate that the inward K^+ current density at -110 mV was significantly enhanced by the application of diazoxide (n=7; $p<0.05$ *vs.* control) and markedly reduced by the addition of glibenclamide (n=5; $p<0.05$ *vs.* diazoxide alone).

JPET Fast Forward. Published on August 6, 2013 as DOI: 10.1124/jpet.113.205138
This article has not been copyedited and formatted. The final version may differ from this version.

The relationship between the membrane potential and $[Ca^{2+}]_i$ in the isolated ciliary cells

The relationship between the membrane potential and $[Ca^{2+}]_i$ was determined in isolated ciliary cells under a whole cell voltage-clamp. The single ciliary cells were loaded with fluo-4 from recording pipettes. A membrane hyperpolarization from -20 to -60 mV induced a slow increase in $[Ca^{2+}]_i$ ($n=4$, $p<0.01$) and the return of the potential to -20 mV removed the increase in $[Ca^{2+}]_i$ completely but at a much slower rate ($n=4$, $p<0.05$; Fig. 6A). The $[Ca^{2+}]_i$ increase induced by hyperpolarization was also abolished by the withdrawal of 2.2 mM Ca^{2+} in the external solution ($n=3$, $p<0.01$; Fig. 6B). As shown in figure 6, the time courses of $[Ca^{2+}]_i$ elevation varied widely from cell to cell, presumably due to the diversity of cell activities after isolation and also the difference in the load of Ca^{2+} indicator among cells. The summarized data indicate that the $[Ca^{2+}]_i$ increase induced by hyperpolarization from -20 to -60 mV was significant, reversible, and susceptible to external Ca^{2+}.

The image analyses of local $[Ca^{2+}]_i$ changes by diazoxide in the ciliary cells

The image analyses of changes in the local $[Ca^{2+}]_i$ were performed using fluo-4/AM and a confocal fluorescent microscope. The changes in the fluorescent intensity of the three areas in the ciliated cell (central, apical, and basolateral areas indicated by “a”, “b” and “c”, respectively in Fig. 7A,a) by the application of 10 μM diazoxide over time were illustrated in Fig. 7A,b. When the intensity at resting conditions in the cell center was taken as unity, the intensities at the apical area and the basolateral area were 1.01±0.01 and 1.00±0.02, respectively ($n=9$, $P>0.05$ among the three areas). After the application of 10 μM diazoxide, the intensities in each area gradually increased (Fig. 7A,b and 7B). The rise in intensity at the apical area was more focal, faster, and larger than the rise in intensity at either the cell center or the basolateral area. The summarized data (Fig. 7C) indicate that the rise in intensity at the cell center was significantly less than the rise in intensity at the apical area ($n=9$, $p<0.05$). The rise in intensity at the basolateral area tended to be smaller than

the rise in intensity at the apical area, but the difference was not significant.

In addition to the focal rise in submembrane area of the apical side (Fig. 7B, ii and iii), Ca^{2+} rise in the cytosol compartments located deep inside the cell was occasionally observed (Fig. 7B, iii, iv and V). This type of Ca^{2+} rise was characteristic of a slow rise, deep-inside location and non-focal or diffused images. This specific rise was observed to varying degrees in 7 out of 9 cells, whereas the focal and rapid Ca^{2+} rises in the apical submembrane areas were clearly detected in all 9 cells examined.

Discussion

Ca^{2+} as one of major factors modulating mucociliary motility

In the ciliary mechanism, the basic mechanism that is responsible for the slow and constitutive rate of beating is considered to be the inherent and spontaneous dynein ATPase activity that depends mainly upon the cellular MgATP concentration (Salathe and Bookman, 1999; Ma et al., 2002). In addition, adapting to the heavier duty of particle transportation with mucus in the epithelium, the up-regulation of the ciliary motility by three separate second messengers have been clarified; 1) Ca^{2+}, 2) c-AMP and 3) c-GMP (Salathe, 2007). The crosstalk among signal pathways by these three second messengers has been also revealed. Among these second messengers, Ca^{2+} has fundamental roles in facilitating CBF (Schmid and Salathe, 2011). The application of a K_{ATP} opener increases the CBF by only 10-15% above the baseline in airway ciliated cells. It has been demonstrated, however, that a 16% increase in CBF results in 56% increase in the mucociliary transport velocity in an isolated trachea (Seybold et al., 1990). In this study, the maximum response to the externally applied physiological stimulants ATP or acetylcholine often resulted in larger rises in $[Ca^{2+}]_i$ than those induced by K_{ATP} openers. These slightly larger increases in CBF (15-30%) suggest that mucociliary clearance may therefore be substantially enhanced by K_{ATP} channel

JPET Fast Forward. Published on August 6, 2013 as DOI: 10.1124/jpet.113.205138
This article has not been copyedited and formatted. The final version may differ from this version.

openers.

New insight into $[Ca^{2+}]_i$ regulation by the membrane potential changes in airway ciliated cells

Information concerning the influence of changes in the membrane potential on the ciliary axoneme movement is not well accumulated and still somewhat controversial. It has been reported that the application of ATP induces $[Ca^{2+}]_i$ rise leading to membrane hyperpolarization and facilitates the ciliary motility in frog palate and esophagus ciliated cells (Tarasiuk et al., 1995). In contrast, it has been reported that the membrane potential changes under the whole cell voltage clamp mode does not induce a significant CBF change in the single airway ciliated cells of the rabbit (Ma et al., 2002). The findings in the present study clearly demonstrated that the membrane hyperpolarization achieved under a voltage clamp or induced by K_{ATP} channel openers elicited $[Ca^{2+}]_i$ rise and resulted in enhanced ciliary axoneme motility in the airway ciliated cells of the mice. The reason for the discrepancy between the studies in rabbit airway ciliated cells (Ma et al., 2002) and our results in mice is not completely clear. The changes in $[Ca^{2+}]_i$ by membrane hyperpolarization under whole cell voltage clamp were not recorded in the former study, presumably because the $[Ca^{2+}]_i$ was fixed by Ca^{2+}-EGTA buffer from the pipette filling solution (Ma et al., 2002). In the present study, the pipette solution contained only 50 μM EGTA and no $CaCl_2$, and the $[Ca^{2+}]_i$ rise by hyperpolarization was consistent and reversible. It is a rather common observation that prolonged membrane hyperpolarization induces a slow but sustained $[Ca^{2+}]_i$ rise in non-excitable cells such as T-lymphocytes, chondrocytes (Funabashi et al., 2010), and vascular endothelial cells (Yamazaki et al., 2011) where the Ca^{2+} permeable channels are functionally expressed but the voltage-gated Ca^{2+} channels are not.

This study differs from the previous, conflicting study (Ma et al., 2002) based on the ATP concentrations used for experimentation. The previous study was conducted using 5 mM MgATP + 0.5 mM K_2ATP, while the current study was conducted using 4 mM $MgCl_2$ + 2 mM Na_2ATP.

Although the basic CBF of inherent and spontaneous beating is considered to be dependent on MgATPase activity, the actual MgATP and ATP concentrations in the airway ciliated cells are unknown. It may be possible that experimental conditions in the present study influenced the CBF increase that were attributed to $[Ca^{2+}]_i$ rise by membrane hyperpolarization induced under voltage-clamp or by application of a K_{ATP} channel opener.

Previous studies have confirmed that the rise of $[Ca^{2+}]_i$ results in CBF enhancement, even if the underlying mechanisms are not fully understood (Schmid and Salathe, 2011). The activation of calmodulin may be involved, as this messenger protein associates with the radial spokes and the central apparatus of the flagella (Dymek and Smith, 2007) and directly interacts with dynein arms (Sakato et al., 2007). These mechanisms have been suggested for correlating the $[Ca^{2+}]_i$ rise with facilitated axoneme motility in invertebrates. Additionally, it has been assumed that the $[Ca^{2+}]_i$ rise facilitates cilia motility via crosstalk with the c-AMP and/or the c-GMP mediated pathways (Braiman and Priel, 2008).

Ca^{2+} source and local Ca^{2+} functions in the regulation of cilia motility

In airway ciliated cells, it has been well established that two major endogenous stimulants, ATP and acetylcholine, activate P_2Y_2 and M_3 receptors, respectively. The stimuli activates phospholipase Cβ to form inositol 1,4,5 trisphosphate (IP_3), which induces $[Ca^{2+}]_i$ release from the endoplasmic reticulum. In addition, it has been recognized that sustained Ca^{2+} influx occurs following Ca^{2+} release. Although the molecular mechanism of the Ca^{2+} influx is not well understood, the store operated and/or receptor operated Ca^{2+} entry may be contributing as it does in many other non-excitable cells. By some stimuli, such as stretch, the transient receptor potential vanilloid subfamily 4 (TRPV4) channel is activated to facilitate Ca^{2+} influx (Lorenzo et al., 2008).

In the present study, it is clearly shown that membrane hyperpolarization by voltage-clamp or the application of a K_{ATP} channel opener facilitates the influx of Ca^{2+}. Since airway epithelial

cells are polarized structures with cilia on their apical membranes, Ca^{2+} concentrations are sufficiently high in the sub-membranous areas to affect ciliary beat (Braiman and Priel, 2008). It has been suggested that storage and release of Ca^{2+} in different cell compartments give rise to this apical versus basolateral concentration difference in the cytosol (Braiman et al., 2000; Braiman and Priel, 2001). In contrast, the measurement of the local $[Ca^{2+}]_i$ in this study did not show a significant Ca^{2+} gradient in the cytosol under the normal conditions (not shown). During membrane hyperpolarization by K_{ATP} openers, the Ca^{2+} rise in the apical submembrane area was significantly higher than that in the center area but not in basolateral area.

In addition to a Ca^{2+} rise in the apical region, diazoxide occasionally induced a slower Ca^{2+} rise in the cytosolic compartments located deep inside the cells. It has been reported that diazoxide interacts with the mitochondrial K_{ATP} channels as well as plasma membrane K_{ATP} channels (Garlid et al., 1996; O'Rourke, 2004). Diazoxide reduces the mitochondrial membrane potential (or induces the mitochondrial depolarization) and thereby accelerates the release of Ca^{2+} from mitochondria (Grimmsmann and Rustenbeck, 1998; Holmuhamedov et al., 1999). In addition to the Ca^{2+} influx mediated by the membrane hyperpolarization, Ca^{2+} release from organelles, including mitochondria, may be involved in the diazoxide-induced Ca^{2+} increase. However, it remains to be determined whether the Ca^{2+} rise induced by diazoxide deep inside the cell compartments contributes to the enhancement of the ciliary movement. Further experiments are therefore required to elucidate the mechanism underlying the local Ca^{2+} mobilization triggered by exposure to diazoxide.

K_{ATP} channels in ciliated cells as a possible therapeutic target

K^+ channels play a major role in maintaining the electrochemical gradient necessary for transepithelial Na^+ and Cl^- transport in secretory airway epithelia (O'Grady and Lee, 2003). The significant contribution of the K_{ATP} channel to lung physiology and pathophysiology has been suggested based on the beneficial actions of openers in the lung (Fukuse et al., 2002). The

JPET Fast Forward. Published on August 6, 2013 as DOI: 10.1124/jpet.113.205138
This article has not been copyedited and formatted. The final version may differ from this version.

molecular components of the K_{ATP} channel in the airway alveolar epithelial type II cells of the rat have been identified as the combination of Kir6.1 and SUR2B (Leroy et al., 2004). A K_{ATP} channel opener induces the relaxation of airway smooth muscle via membrane hyperpolarization and the subsequent suppression of voltage-dependent Ca^{2+} channel (VDCC) activity (Rodrigo and Standen, 2005). This relaxation is considered to be effective for the therapy of occlusive diseases such as asthma and chronic occlusive pulmonary disease (COPD) (Pelaia et al., 2002).

In this study, two K_{ATP} channel openers, diazoxide and pinacidil and a blocker, glibenclamide were used as pharmacological tools to determine the subunits responsible for K_{ATP} channel in mouse ciliated cells. The combination of K_{ATP} channel subunits modulates sensitivity to K_{ATP} channel openers. Diazoxide activates SUR1 and SUR2B but not SUR2A (Yamada and Kurachi, 2005). On the other hand, pinacidil activates SUR2A and SUR2B but not SUR1. Because K_{ATP} channels in ciliated cells were activated by both diazoxide and pinacidil at < 10 μM (Hibino et al., 2010), functional K_{ATP} channels in these cells are supposed to be Kir6.x/SUR2B. These results were supported by the outcomes from RT-PCR analyses and immunocytochemical staining, which showed the expression of Kir6.1, Kir6.2 and SUR2B on plasma membrane. Interestingly, immunostaining using anti-SUR1 revealed that SUR1 subunits were specifically located on cilia, but neither Kir6.1 nor Kir6.2 was detected there. SUR1 may possibly couple with other ion channels such as TRP channel (Woo et al., 2013). Unfortunately, the strategy of molecular manipulation by use of siRNA did not fit to this study, because rat cilia disappear during cell culture for 2 days (Chang et al., 1985) and the results were confirmed using mouse cilia in this study. Therefore, it remained to be determined whether Kir6.1 or kir6.2 is functionally predominant subunit in ciliated cells, while Kir6.2 protein expression on the plasma membrane appeared to be higher than Kir6.1.

Membrane potential recording with $DiBAC_4(3)$ allows us to get more number of results than the direct recordings under whole cell patch clamp configuration. However, the use of

$DiBAC_4(3)$ has at least three limitations. One is the artifacts by $DiBAC_4(3)$ as a potent activator of large-conductance Ca^{2+}-activated K^+ channel (BK channel) (Morimoto et al., 2007). BK channel current component sensitive to paxilline was not recorded in ciliary cells. The second limitation is that $DiBAC_4(3)$ cannot detect fast membrane potential changes. The third and the most serious one is that the exact membrane potential can not be measured by $DiBAC_4(3)$, even though calibration under voltage-clamp is available (Yamada et al., 2001). The membrane hyperpolarization induced by 10 μM diazoxide appeared to be approximately 11 mV, based on the calibration. This value was apparently larger than that directly recorded under current clamp mode (4 mV). The reason for the dissociation between two measurements is not clear. It is, however, likely that the Cl^- conductance appears to be high in comparison with that of K^+ in ciliated cells. When the pipette filling solution contained 140 mM Cl^-, the resting membrane potential was extremely shallow (-19 mV) and close to equilibrium potential of Cl^- rather than K^+. Under these experimental conditions, the membrane hyperpolarization due to the K^+ conductance increase may be smaller than that occurs under normal Cl^- gradient across the cell membrane. The intracellular Cl^- concentration varied widely depending on cell types in a range of 5 and 30 mM, but is unfortunately unknown in tracheal ciliated cells. Further study is required to understand the real membrane hyperpolarization by K_{ATP} channel opening in ciliary cells.

In this study, the membrane hyperpolarization increased the influx of Ca^{2+} presumably by an unknown pathway rather than by VDCC. The membrane hyperpolarization may simply increase the transmembrane driving force for Ca^{2+} through Ca^{2+} permeable channels with non-voltage dependent gating mechanisms. Taken together, it can be suggested that K_{ATP} channel openers may have additional benefits, including an expectorant effect, for the therapy of occlusive respiratory disorders.

In conclusion, a K_{ATP} channel composed of Kir6.2/SUR2B and possibly also Kir6.1/SUR2B are functionally expressed in ciliated cells in mice airway epithelium. The activation of a K_{ATP} channel induces membrane hyperpolarization and results in an increase in Ca^{2+}-influx

JPET Fast Forward. Published on August 6, 2013 as DOI: 10.1124/jpet.113.205138
This article has not been copyedited and formatted. The final version may differ from this version.

through a novel, non-VDCC pathway. The enhancement of the ciliary movement by K_{ATP} openers is mainly attributable to the Ca^{2+} rise and is considered to have an additional and beneficial effect on the current drug therapies used to treat occlusive respiratory disorders.

Authorship contributions

Participated in the research design: Ohba, Sawada, and Imaizumi.

Conducted the experiments: Ohba, Sawada and Suzuki.

Performed the data analysis: Ohba, Sawada, Yamamura, Ohya, and Imaizumi.

Wrote or contributed to the writing of the manuscript: Tsuda and Imaizumi.

References

Braiman A, Gold'Shtein V and Priel Z (2000) Feasibility of a sustained steep Ca(2+)Gradient in the cytosol of electrically non-excitable cells. *Journal of theoretical biology* **206**:115-130.

Braiman A and Priel Z (2001) Intracellular stores maintain stable cytosolic Ca(2+) gradients in epithelial cells by active Ca(2+) redistribution. *Cell calcium* **30**:361-371.

Braiman A and Priel Z (2008) Efficient mucociliary transport relies on efficient regulation of ciliary beating. *Respiratory physiology & neurobiology* **163**:202-207.

Chang LY, Wu R and Nettesheim P (1985) Morphological changes in rat tracheal cells during the adaptive and early growth phase in primary cell culture. *Journal of cell science* **74**:283-301.

Clark R and Proks P (2010) ATP-sensitive potassium channels in health and disease. *Advances in experimental medicine and biology* **654**:165-192.

Dymek EE and Smith EF (2007) A conserved CaM- and radial spoke associated complex mediates regulation of flagellar dynein activity. *The Journal of cell biology* **179**:515-526.

Evans JH and Sanderson MJ (1999) Intracellular calcium oscillations regulate ciliary beat frequency of airway epithelial cells. *Cell calcium* **26**:103-110.

Flagg TP, Enkvetchakul D, Koster JC and Nichols CG (2010) Muscle KATP channels: recent insights to energy sensing and myoprotection. *Physiological reviews* **90**:799-829.

Fukuse T, Hirata T, Omasa M and Wada H (2002) Effect of adenosine triphosphate-sensitive potassium channel openers on lung preservation. *American journal of respiratory and critical care medicine* **165**:1511-1515.

Funabashi K, Ohya S, Yamamura H, Hatano N, Muraki K, Giles W and Imaizumi Y (2010) Accelerated Ca2+ entry by membrane hyperpolarization due to Ca2+-activated K+ channel activation in response to histamine in chondrocytes. *American journal of physiology Cell physiology* **298**:C786-797.

Garlid KD, Paucek P, Yarov-Yarovoy V, Sun X and Schindler PA (1996) The mitochondrial KATP channel as a receptor for potassium channel openers. *The*

Journal of biological chemistry **271**:8796-8799.

Grimmsmann T and Rustenbeck I (1998) Direct effects of diazoxide on mitochondria in pancreatic B-cells and on isolated liver mitochondria. *British journal of pharmacology* **123**:781-788.

Hibino H, Inanobe A, Furutani K, Murakami S, Findlay I and Kurachi Y (2010) Inwardly rectifying potassium channels: their structure, function, and physiological roles. *Physiological reviews* **90**:291-366.

Holmuhamedov EL, Wang L and Terzic A (1999) ATP-sensitive K+ channel openers prevent Ca2+ overload in rat cardiac mitochondria. *The Journal of physiology* **519 Pt 2**:347-360.

Imaizumi Y, Muraki K and Watanabe M (1989) Ionic currents in single smooth muscle cells from the ureter of the guinea-pig. *The Journal of physiology* **411**:131-159.

Leroy C, Dagenais A, Berthiaume Y and Brochiero E (2004) Molecular identity and function in transepithelial transport of K(ATP) channels in alveolar epithelial cells. *American journal of physiology Lung cellular and molecular physiology* **286**:L1027-1037.

Lorenzo IM, Liedtke W, Sanderson MJ and Valverde MA (2008) TRPV4 channel participates in receptor-operated calcium entry and ciliary beat frequency regulation in mouse airway epithelial cells. *Proceedings of the National Academy of Sciences of the United States of America* **105**:12611-12616.

Ma W, Silberberg SD and Priel Z (2002) Distinct axonemal processes underlie spontaneous and stimulated airway ciliary activity. *The Journal of general physiology* **120**:875-885.

Malerba M, Radaeli A, Mancuso S and Polosa R (2010) The potential therapeutic role of potassium channel modulators in asthma and chronic obstructive pulmonary disease. *Journal of biological regulators and homeostatic agents* **24**:123-130.

Morimoto T, Sakamoto K, Sade H, Ohya S, Muraki K and Imaizumi Y (2007) Voltage-sensitive oxonol dyes are novel large-conductance Ca2+-activated K+ channel activators selective for beta1 and beta4 but not for beta2 subunits. *Molecular pharmacology* **71**:1075-1088.

O'Grady SM and Lee SY (2003) Chloride and potassium channel function in alveolar epithelial cells. *American journal of physiology Lung cellular and molecular*

physiology **284**:L689-700.

O'Rourke B (2004) Evidence for mitochondrial K+ channels and their role in cardioprotection. *Circulation research* **94**:420-432.

Pelaia G, Gallelli L, Vatrella A, Grembiale RD, Maselli R, De Sarro GB and Marsico SA (2002) Potential role of potassium channel openers in the treatment of asthma and chronic obstructive pulmonary disease. *Life sciences* **70**:977-990.

Rodrigo GC and Standen NB (2005) ATP-sensitive potassium channels. *Current pharmaceutical design* **11**:1915-1940.

Sakato M, Sakakibara H and King SM (2007) Chlamydomonas outer arm dynein alters conformation in response to Ca2+. *Molecular biology of the cell* **18**:3620-3634.

Salathe M (2007) Regulation of mammalian ciliary beating. *Annual review of physiology* **69**:401-422.

Salathe M and Bookman RJ (1999) Mode of Ca2+ action on ciliary beat frequency in single ovine airway epithelial cells. *The Journal of physiology* **520 Pt 3**:851-865.

Schmid A and Salathe M (2011) Ciliary beat co-ordination by calcium. *Biology of the cell / under the auspices of the European Cell Biology Organization* **103**:159-169.

Seybold ZV, Mariassy AT, Stroh D, Kim CS, Gazeroglu H and Wanner A (1990) Mucociliary interaction in vitro: effects of physiological and inflammatory stimuli. *Journal of applied physiology* **68**:1421-1426.

Tarasiuk A, Bar-Shimon M, Gheber L, Korngreen A, Grossman Y and Priel Z (1995) Extracellular ATP induces hyperpolarization and motility stimulation of ciliary cells. *Biophysical journal* **68**:1163-1169.

Trinh NT, Prive A, Kheir L, Bourret JC, Hijazi T, Amraei MG, Noel J and Brochiero E (2007) Involvement of KATP and KvLQT1 K+ channels in EGF-stimulated alveolar epithelial cell repair processes. *American journal of physiology Lung cellular and molecular physiology* **293**:L870-882.

Trinh NT, Prive A, Maille E, Noel J and Brochiero E (2008) EGF and K+ channel activity control normal and cystic fibrosis bronchial epithelia repair. *American journal of physiology Lung cellular and molecular physiology* **295**:L866-880.

Weiss T, Gheber L, Shoshan-Barmatz V and Priel Z (1992) Possible mechanism of

ciliary stimulation by extracellular ATP: involvement of calcium-dependent potassium channels and exogenous Ca2+. *The Journal of membrane biology* **127**:185-193.

Woo SK, Kwon MS, Ivanov A, Gerzanich V and Simard JM (2013) The sulfonylurea receptor 1 (Sur1)-transient receptor potential melastatin 4 (Trpm4) channel. *The Journal of biological chemistry* **288**:3655-3667.

Yamada A, Gaja N, Ohya S, Muraki K, Narita H, Ohwada T and Imaizumi Y (2001) Usefulness and limitation of DiBAC4(3), a voltage-sensitive fluorescent dye, for the measurement of membrane potentials regulated by recombinant large conductance Ca2+-activated K+ channels in HEK293 cells. *Japanese journal of pharmacology* **86**:342-350.

Yamada M and Kurachi Y (2005) A functional role of the C-terminal 42 amino acids of SUR2A and SUR2B in the physiology and pharmacology of cardiovascular ATP-sensitive K(+) channels. *Journal of molecular and cellular cardiology* **39**:1-6.

Yamamura H, Ikeda C, Suzuki Y, Ohya S and Imaizumi Y (2012) Molecular assembly and dynamics of fluorescent protein-tagged single KCa1.1 channel in expression system and vascular smooth muscle cells. *American journal of physiology Cell physiology* **302**:C1257-1268.

Yamazaki D, Kito H, Yamamoto S, Ohya S, Yamamura H, Asai K and Imaizumi Y (2011) Contribution of K(ir)2 potassium channels to ATP-induced cell death in brain capillary endothelial cells and reconstructed HEK293 cell model. *American journal of physiology Cell physiology* **300**:C75-86.

Footnotes

Authors

TO and ES contributed equally to this study.

Grants

This investigation was supported by a Grant-in-Aid for Scientific Research on Priority Areas (23136512 to Y.I.) from the Ministry of Education, Culture, Sports, Science, and Technology in Japan, and by Grant-in-Aids for Scientific Research (B) (23390020 to Y.I.) from the Japan Society for the Promotion of Science. This work was also supported by Health and Labor Sciences Research Grants by the Ministry of Health, Labor and Welfare, Japan (Research on Risk of Chemical Substance 21340601, H19-kagaku-ippan-006 and H22-kagaku-ippan-005 to HT).

Reprint request

Yuji Imaizumi, Ph.D.

Department of Molecular and Cellular Pharmacology

Graduate School of Pharmaceutical Sciences

Nagoya City University

3-1 Tanabedori, Mizuhoku, Nagoya 467-8603, Japan

TEL & FAX: +81-52-836-3431

E-mail: yimaizum@phar.nagoya-cu.ac.jp

Legends for Figures

Figure 1. The enhancement of the ciliary movement by diazoxide

A: The ciliary movement in an epithelial cell isolated from a mouse trachea was recorded with a high speed digital camera at 100 Hz. The ciliary beating frequency (CBF) was directly measured from the images as shown by the dotted and solid lines. The series of images (a, b and c) were obtained at the time shown in B.

B: The time course of CBF in HEPES-buffered solution, in the presence of 10 μM diazoxide (Diaz), and following the addition of 5 μM glibenclamide (Glib).

C: The summarized data concerning the effects of diazoxide and glibenclamide (n=6), *,** $p<0.05$ and 0.01, respectively.

Figure 2. The diazoxide-induced hyperpolarization of the membrane.

A: The changes in the membrane potential were monitored by the voltage-sensitive dye $DiBAC_4(3)$. The changes in the fluorescent intensity ratio (F/F_0) that were induced by the addition of 10 μM diazoxide (Diaz) and 5 μM glibenclamide (Glib) were plotted against time (a). The average fluorescent intensity (F) measured immediately prior to the application of the diazoxide was taken as F_0. The summarized data concerning F/F_0 were shown in "b" (n=5). *, ** $p<0.05$ and 0.01, respectively.

B: The changes in F/F_0 that were induced by the cumulative additions of diazoxide in a dose range from 1 to 30 μM were plotted against time (a). The summarized data concerning F/F_0 were shown in "b" (n=11).

The EC_{50} value and Hill coefficient were 2.3 μM and 3.4, respectively.

Figure 3. The effects of diazoxide and glibenclamide on $[Ca^{2+}]_i$ in ciliated cells.

A: $[Ca^{2+}]_i$ was measured as fluorescent intensity ratio (*340/380*) in a ciliated cell that was loaded

with fura-2/AM. The changes in the ratio induced by the addition of 10 μM diazoxide (Diaz) and 5 μM glibenclamide (Glib) were plotted against time (a). The summarized data concerning the changes in F/F_0 were shown in "b" (n=8). The averaged ratio immediately prior to the application of diazoxide was taken as 1.0. **p< 0.01.

B: The changes in the ratio induced by the addition of 10 μM pinacidil (Pina) and 5 μM glibenclamide were plotted against time (a). The summarized data concerning the changes in F/F_0 were shown in "b" (n=5). The averaged ratio immediately prior to the application of the diazoxide was taken as 1.0. **p<0.01.

Figure 4. The expression of K_{ATP} channel mRNA and the K_{ATP} current in the ciliated cells.

A: The expression of Kir6.x and SURx in the ciliated cells was examined by multi-cell RT-PCR. Approximately 40 of the isolated ciliated cells in which ciliary movement was detected were collected by small pipettes in microscopic fields. Reaction solution from which RTase was omitted was used as a negative control. The expression of the transcripts for Kir6.1, Kir6.2 and SUR2 was detected. Further analyses suggest that the major transcript of SUR2 was SUR2B.

B: The protein expression was detected using immunocytochemical staining. Similarly to the results from RT-PCR, Kir6.1, Kir6.2 and SUR2B, not SUR2A, were expressed on cell surface. SUR1 exhibited specific expression on cilia. The lower sets of panels indicate that the specific staining was prevented by a corresponding inhibitory peptide.

Figure 5. K_{ATP} current in ciliated cells.

A: The membrane currents were measured from a single ciliary cell under a voltage-clamp. A ramp pulse from +40 to -120 mV (as indicated in inset) was applied in the absence (control) and the presence of 10 μM diazoxide (Diaz) and following the addition of 5 μM glibenclamide (Glib). The I-V relationships were obtained by the ramp pulse protocol. The I-V relationships in the presence of

diazoxide with the absence and presence of glibenclamide crossed at -33 mV.

B: The data concerning the current density at -110 mV were summarized. The numbers of experiments were 7 in the control, 7 in the presence of diazoxide and 5 in the co-presence of glibenclamide. *p<0.05.

Figure 6. $[Ca^{2+}]_i$ changes induced by the membrane hyperpolarization in ciliary the cells under a voltage-clamp.

A: The changes in $[Ca^{2+}]_i$ were monitored with the F/F_0 of the fluo4 that was applied from the recording pipette. The time course of F/F_0 during the membrane potential changes from -20 mV to -60 mV and back to -20 mV was plotted against time (a). The top trace indicates the clamp potential changes. The summarized data concerning F/F_0 at -20 mV, at -60 mV and back to -20 mV were shown in "b" (n=4). *, **p<0.05 and 0.01, respectively.

B: The effect of Ca^{2+} removal from an external solution on the elevated F/F_0 by the hyperpolarization of the membrane was examined in a ciliary cell under a voltage clamp.

The external solution was exchanged from the standard solution (2.2 mM Ca^{2+}) to a Ca^{2+} free solution (0 mM Ca^{2+}) at a potential of -60 mV as indicated in the top trace. The summarized data concerning F/F_0 at -20 mV, at -60 mV, and following the exposure to a Ca^{2+} free solution were shown in "b" (n=4). *, **p<0.05 and 0.01, respectively.

Figure 7. The image analyses of local Ca^{2+} transients induced by diazoxide in the ciliary cells.

A: The local Ca^{2+} transients were measured by confocal fluorescent microscopy. The F/F_0 signals of fluo-4 were measured in the three areas indicated in the transfer image of the ciliary cell (left panel): "a" (center of the cell). "b" (apical submembrane area), and "c" (basolateral submembrane area). In the right panel, changes in F/F_0 in the three areas were plotted against time. The F_0 in area "a" was taken as 1.0 and F/F_0 in the other areas was normalized by the F_0.

B: The confocal images of $[Ca^{2+}]_i$ were obtained from the ciliary cell in the absence (i) and presence (ii, iii, and iv) of diazoxide at the timing shown in “A,b”.

C: The summarized data concerning $\Delta F/F_0$ were obtained as the differences of F/F_0 in the absence and presence of diazoxide in “A, right panel” (n=9). * $p < 0.05$.

Fig.1

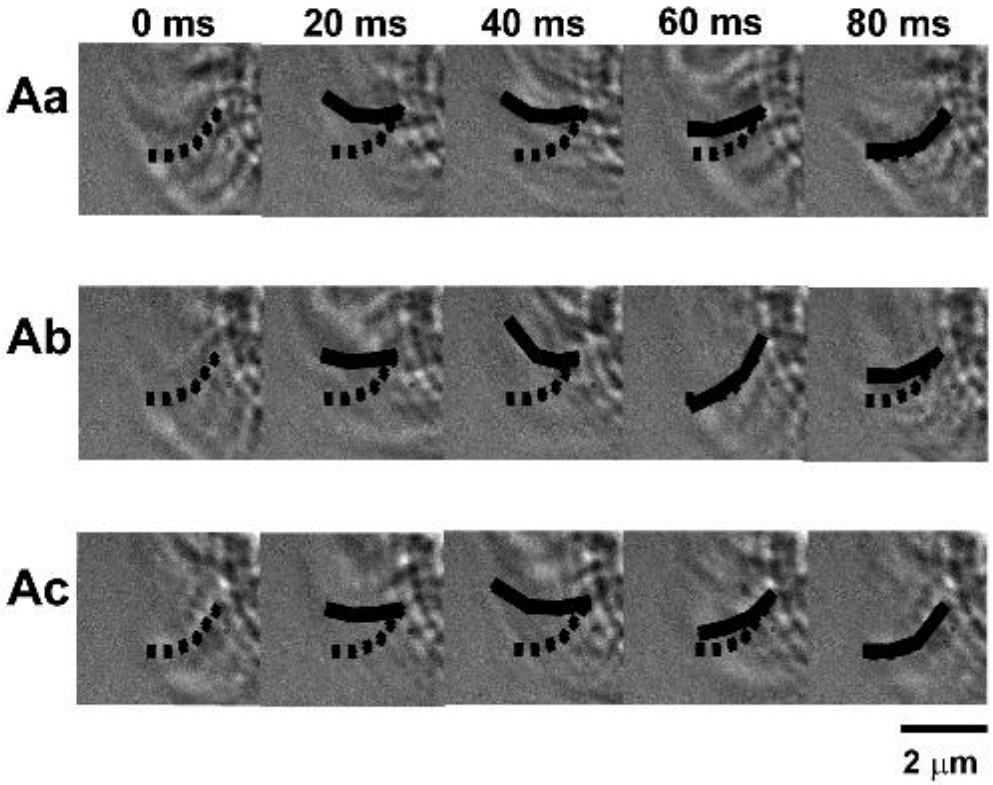
0 ms
20 ms
40 ms
60 ms
80 ms
Aa
Ab
Ac
2 μm

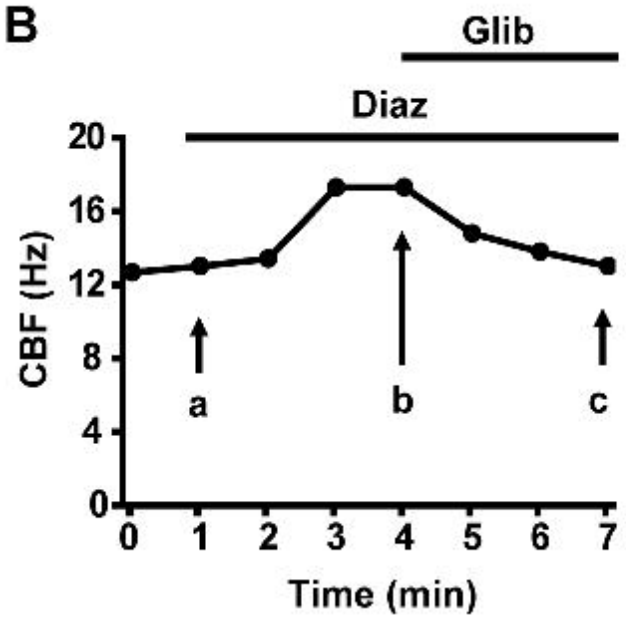
B
Glib
Diaz
20
16
12
8
4
0
CBF (Hz)
a
b
c
0
1
2
3
4
5
6
7
Time (min)

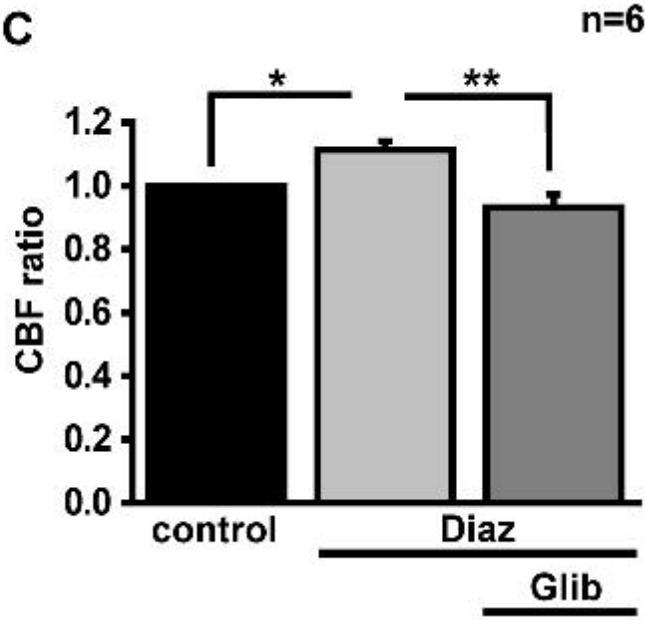
C
n=6
*
**
1.2
1.0
0.8
0.6
0.4
0.2
0.0
CBF ratio
control
Diaz
Glib

Fig.2

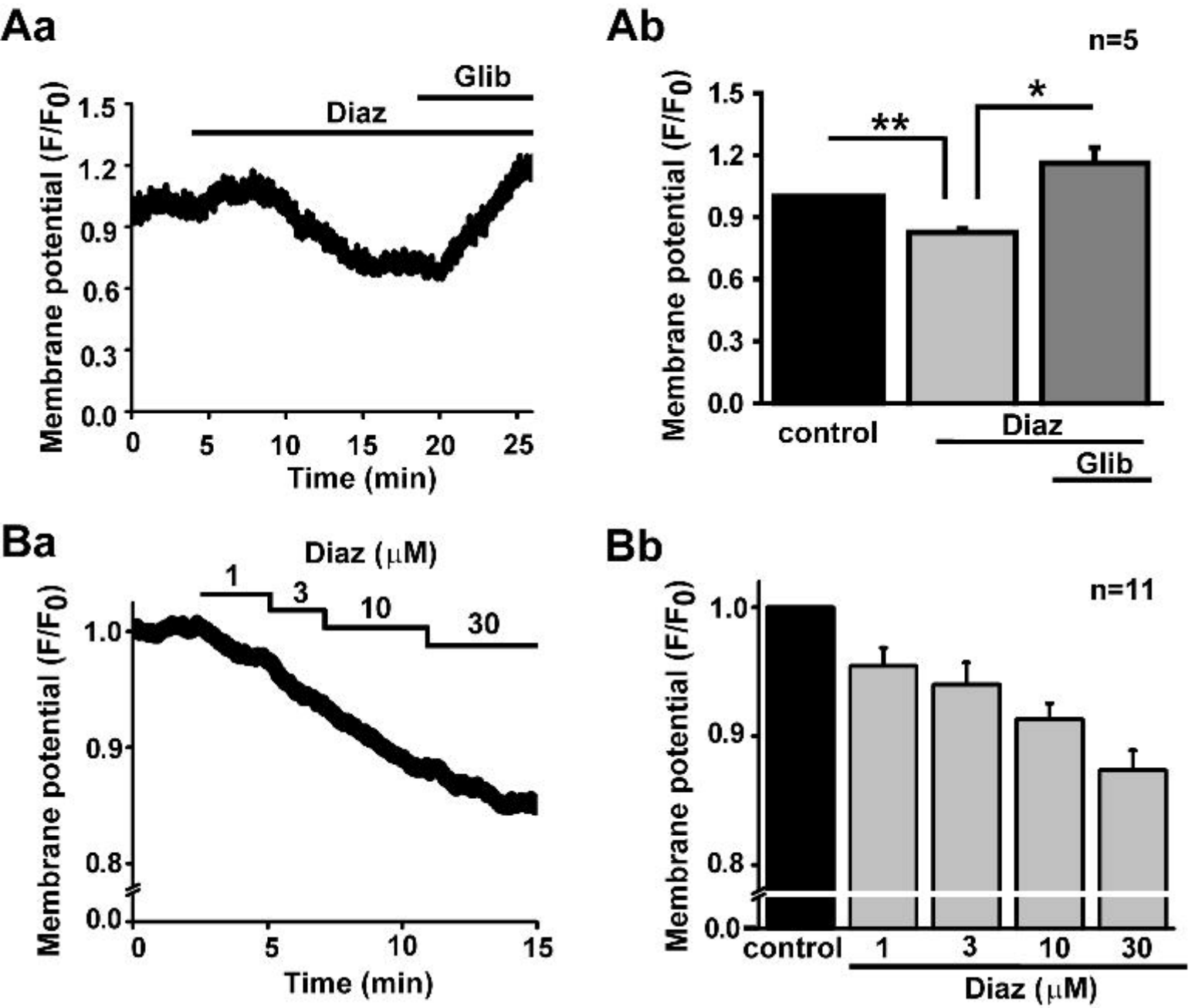
Aa
Glib
Diaz
Membrane potential (F/F0)
1.5
1.2
0.9
0.6
0.3
0.0
0
5
10
15
20
25
Time (min)
Ab
n=5
**
*
Membrane potential (F/F0)
1.5
1.2
0.9
0.6
0.3
0.0
control
Diaz
Glib
Ba
Diaz (μM)
1
3
10
30
Membrane potential (F/F0)
1.0
0.9
0.8
0.0
0
5
10
15
Time (min)
Bb
n=11
Membrane potential (F/F0)
1.0
0.9
0.8
0.0
control
1
3
10
30
Diaz (μM)

Fig.3

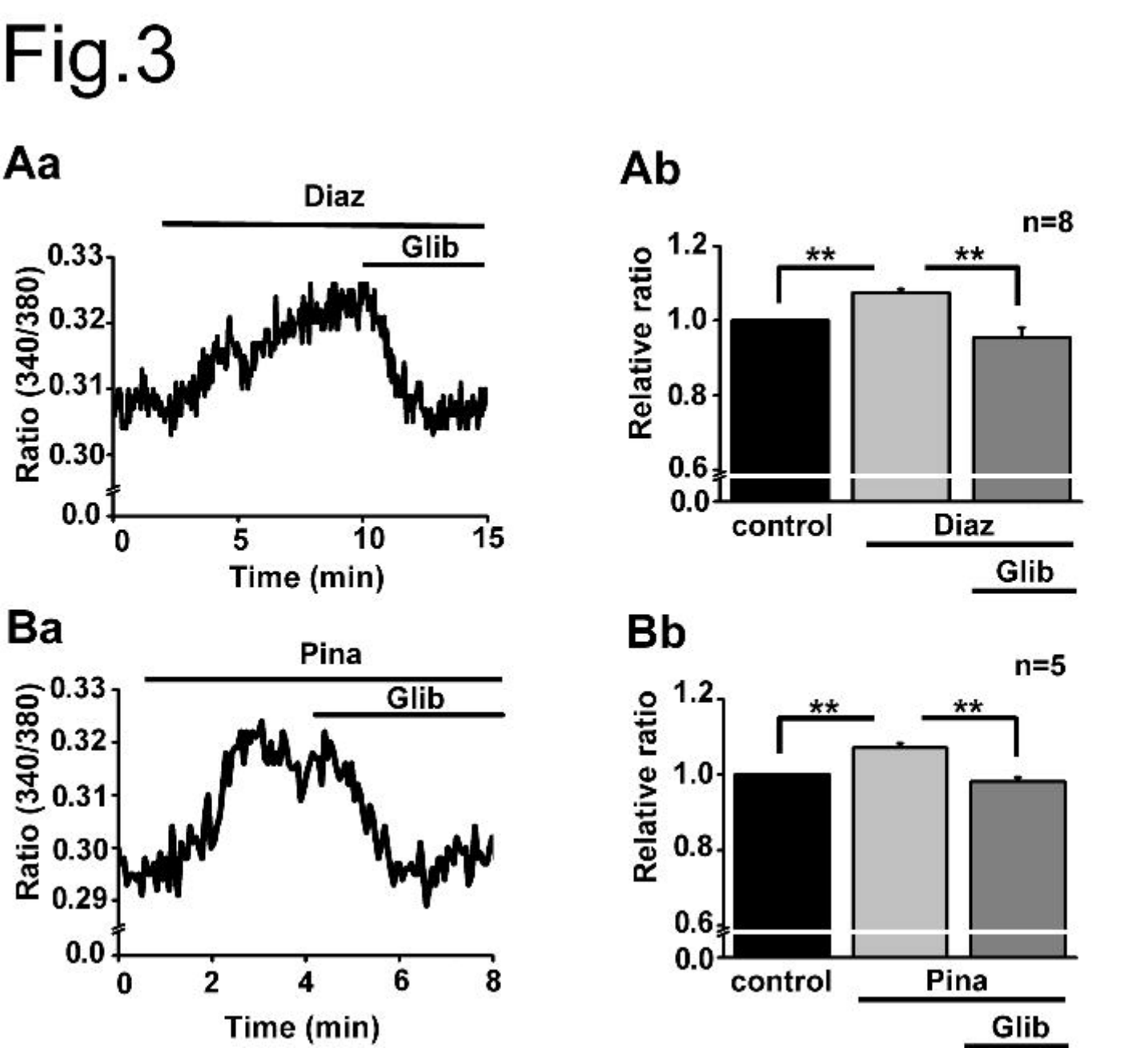
Aa
Diaz
Glib
Ratio (340/380)
0.33
0.32
0.31
0.30
0.0
0
5
10
15
Time (min)
Ab
n=8
Relative ratio
1.2
1.0
0.8
0.6
0.0
**
**
control
Diaz
Glib
Ba
Pina
Glib
Ratio (340/380)
0.33
0.32
0.31
0.30
0.29
0.0
0
2
4
6
8
Time (min)
Bb
n=5
Relative ratio
1.2
1.0
0.8
0.6
0.0
**
**
control
Pina
Glib

Fig.4

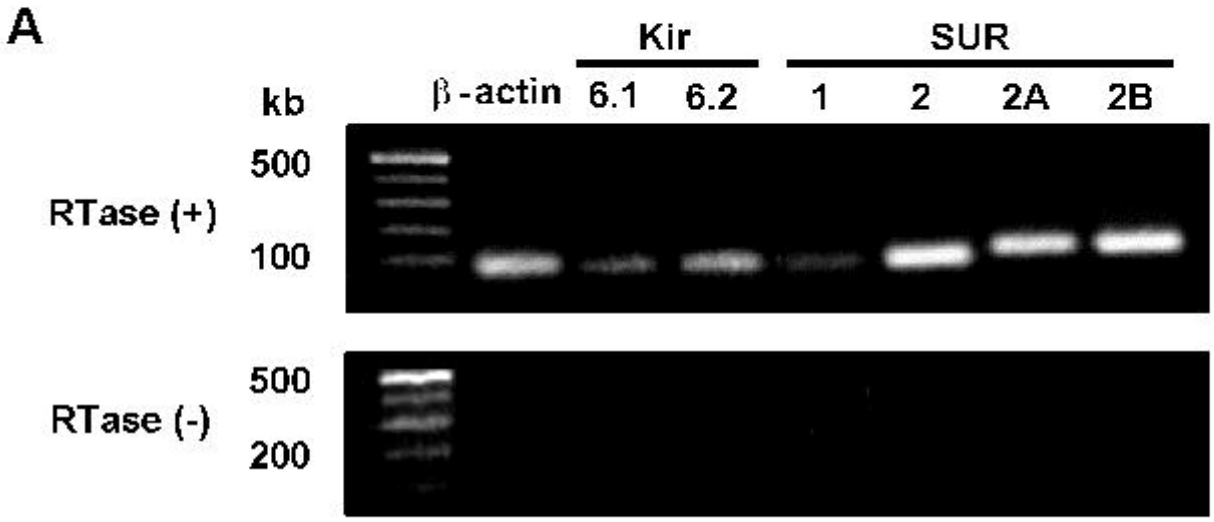
A
Kir
SUR
kb
β-actin
6.1
6.2
1
2
2A
2B
500
100
RTase (+)
500
200
RTase (-)

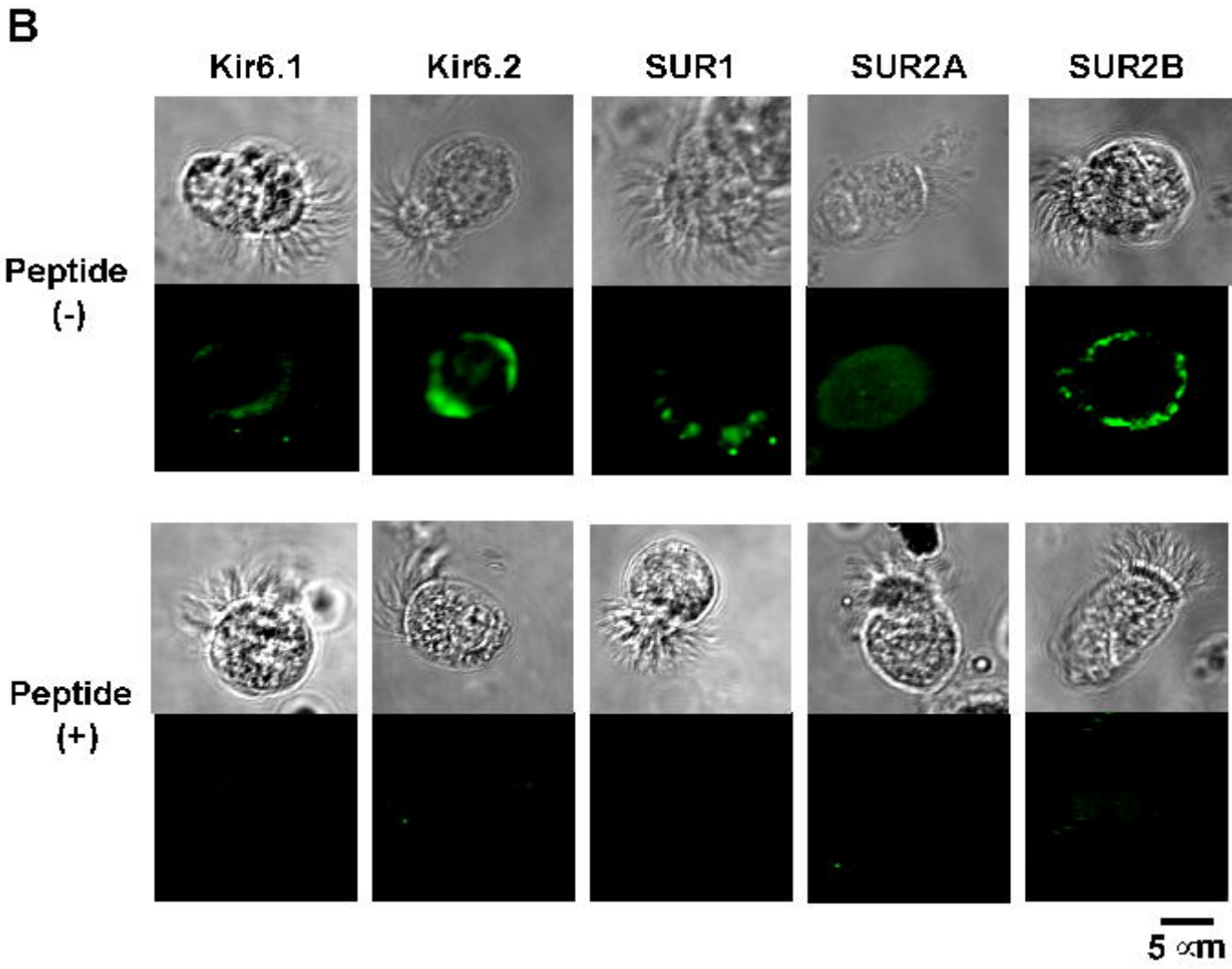
B
Kir6.1
Kir6.2
SUR1
SUR2A
SUR2B
Peptide (-)
Peptide (+)
5 ∝m

Fig.5

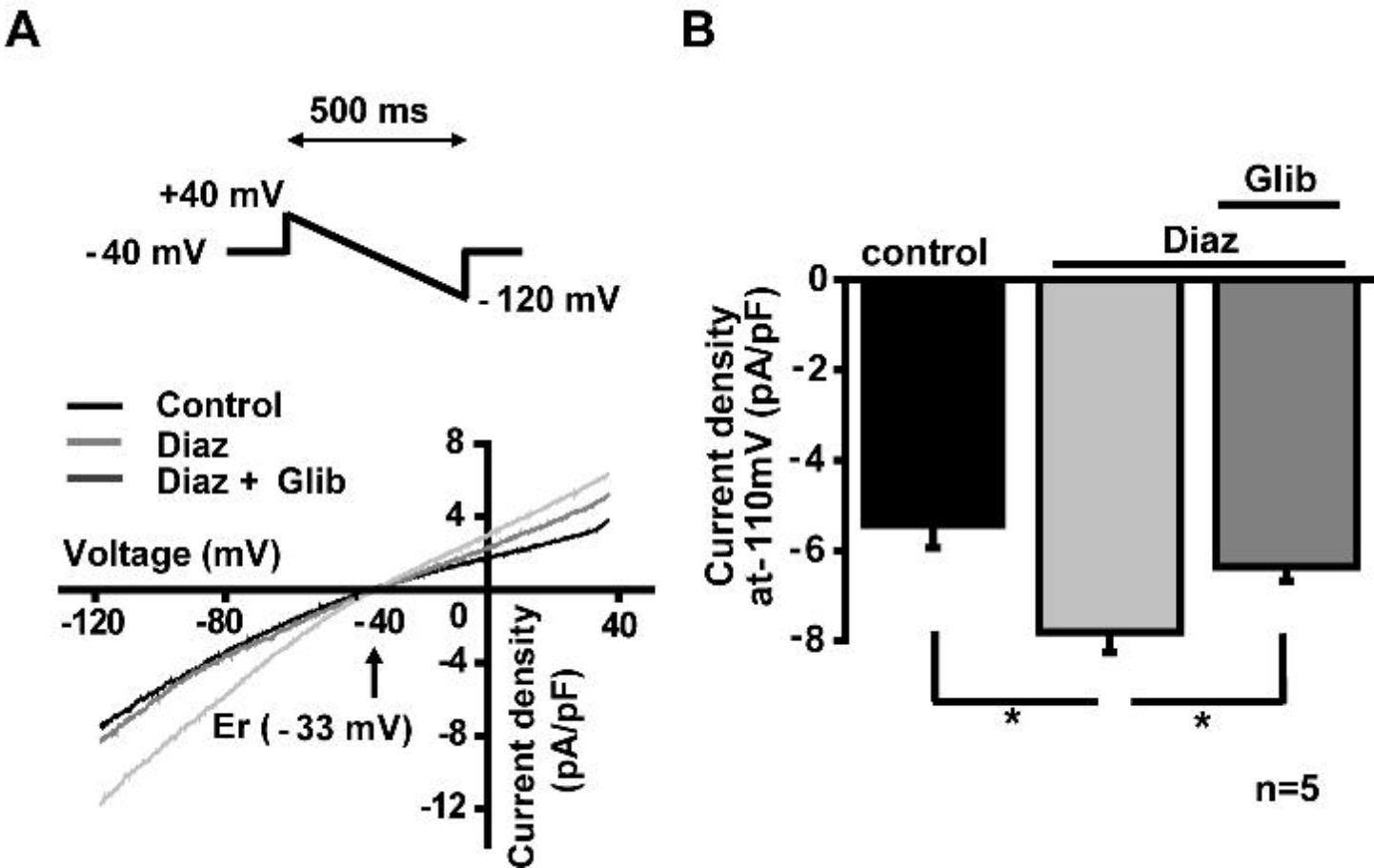
A
500 ms
+40 mV
-40 mV
-120 mV
Control
Diaz
Diaz + Glib
Voltage (mV)
-120
-80
-40
0
40
8
4
-4
-8
-12
Er (-33 mV)
Current density (pA/pF)
B
Glib
control
Diaz
Current density at-110mV (pA/pF)
0
-2
-4
-6
-8
*
*
n=5

Fig.6

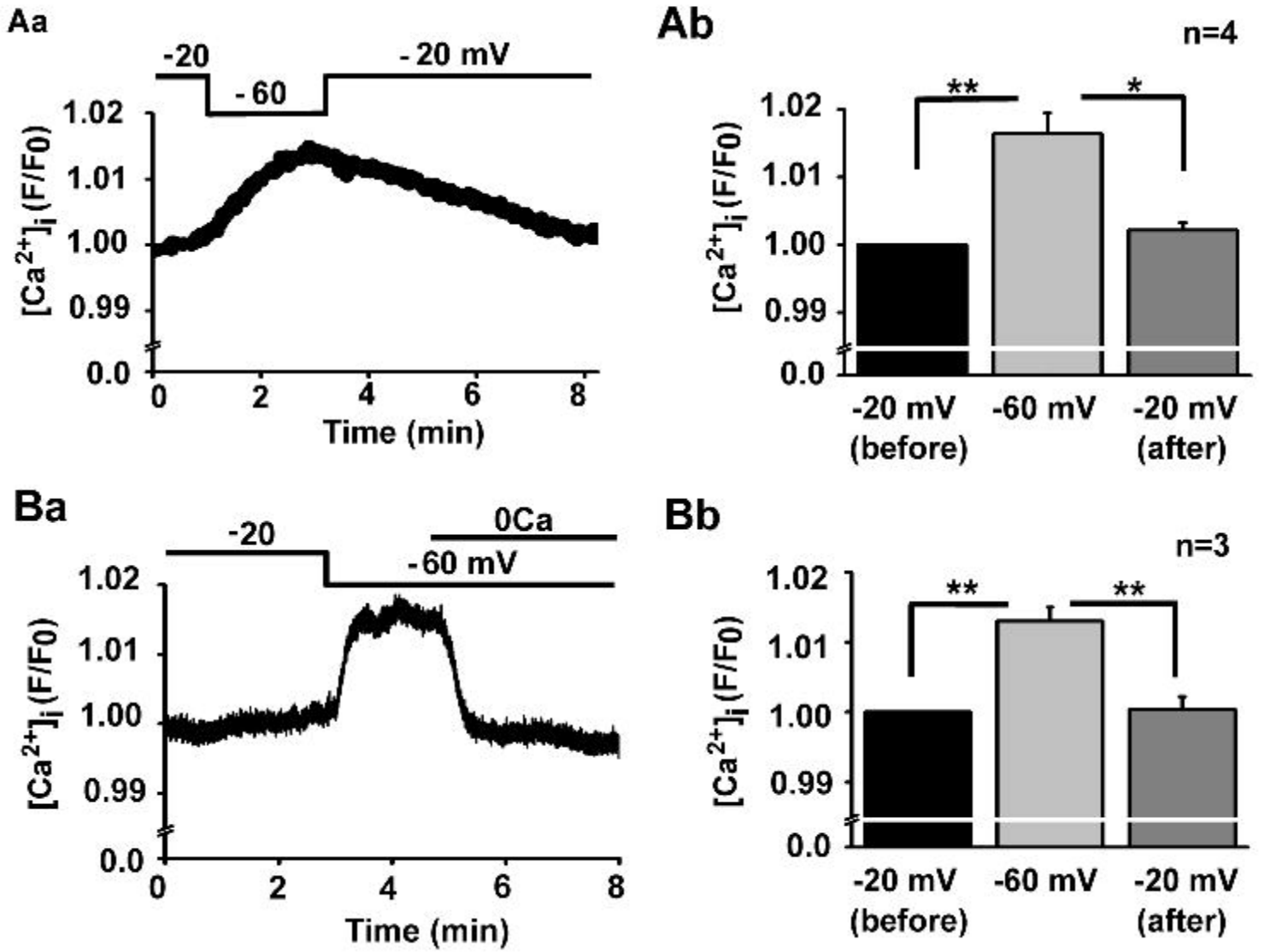
Aa
-20
- 60
- 20 mV
1.02
1.01
1.00
0.99
0.0
[Ca2+]i (F/F0)
0
2
4
6
8
Time (min)
Ab
n=4
**
*
1.02
1.01
1.00
0.99
0.0
[Ca2+]i (F/F0)
-20 mV
(before)
-60 mV
-20 mV
(after)
Ba
-20
0Ca
-60 mV
1.02
1.01
1.00
0.99
0.0
[Ca2+]i (F/F0)
0
2
4
6
8
Time (min)
Bb
n=3
**
**
1.02
1.01
1.00
0.99
0.0
[Ca2+]i (F/F0)
-20 mV
(before)
-60 mV
-20 mV
(after)

Fig.7

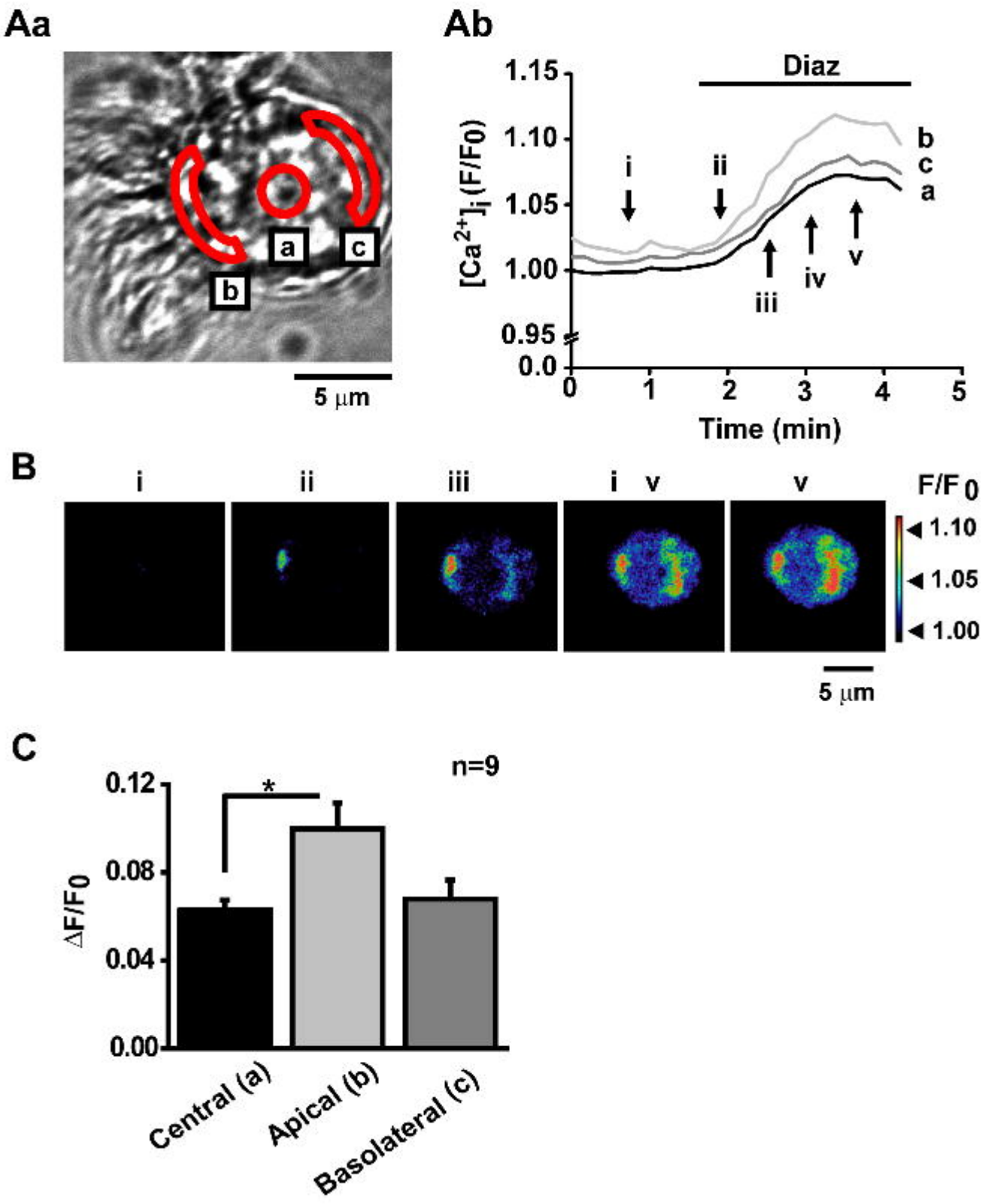
Aa
a
b
c
5 μm
Ab
Diaz
1.15
1.10
1.05
1.00
0.95
0.0
$[Ca^{2+}]_i$ (F/F0)
i
ii
iii
iv
v
b
c
a
0
1
2
3
4
5
Time (min)
B
i
ii
iii
i v
v
F/F 0
1.10
1.05
1.00
5 μm
C
n=9
*
0.12
0.08
0.04
0.00
ΔF/F0
Central (a)
Apical (b)
Basolateral (c)